
Dynamic Responses of Liquid Storage Tank Under Near Fault Pulse-Like Earthquakes With Different Focal Mechanisms

Wei Jing

Key Laboratory of Earthquake Engineering and Engineering Vibration, Institute of Engineering Mechanics, China Earthquake Administration.

Western Engineering Research Center of Disaster Mitigation in Civil Engineering of Ministry of Education, Lanzhou University of Technology, Lanzhou, 730050, PR China.

Ningxia Center for Research on Earthquake Protection and Disaster Mitigation in Civil Engineering, Ningxia University, Ningxia, 750021, PR China. E-mail: jingwei3276@163.com

Jian Shen and Xuansheng Cheng

Western Engineering Research Center of Disaster Mitigation in Civil Engineering of Ministry of Education, Lanzhou University of Technology, Lanzhou, 730050, PR China.

(Received 26 November 2021; accepted 26 January 2022)

A liquid storage tank has a very extensive role in the petrochemical industry, and earthquake damage will cause very serious consequences. Considering the fluid-solid coupling, material nonlinearity and liquid level shaking dynamic behavior, three-dimensional calculation models of non-isolated and isolated liquid storage tanks are established, respectively. 12 earthquake waves are selected from Pacific Earthquake Engineering Research Center (PEER), and there are three earthquake waves of reverse (R), strike slip (SS), reverse oblique (RO) and normal (N) focal mechanisms, respectively. The influence of the focal mechanism on the dynamic responses of the liquid storage tank is investigated. The effectiveness control of sliding isolation on a near fault earthquake is discussed. The influence of the diameter of the limiting device on the shock absorption effect is analyzed. The results show that the order of influence of four types of focal mechanisms on liquid sloshing wave height is as follows: $RO > R > SS > N$. For the wall displacement, liquid pressure and effective stress of the tank wall, the response under N-type focal mechanism earthquake is generally larger than that of the other three types, and the difference of wall displacement, liquid pressure and wall effective stress under RO, R and SS focal mechanism earthquakes is small. The results show that the dynamic responses of the liquid storage tank under different focal mechanism earthquakes is quite different. Sliding isolation can significantly reduce the dynamic responses of the liquid storage tank under strong near-fault earthquakes, and the diameter of the limiting device will affect the shock absorption effect of sliding isolation.

1. INTRODUCTION

When compared with a far-fault earthquake, a near-fault earthquake has the characteristics of a directional effect, high velocity pulse and large vertical acceleration of fault rupture. These characteristics may increase the seismic responses of the structure, thus having more adverse effects on the structure and even aggravating the damage of the structure. Pan et al.¹ studied the seismic response of long-term high-rise isolated structures under the action of a near-fault pulse-like earthquake, and it was found that LRB isolation system would fail due to deformation overrun under the near fault rare earthquake. Du et al.² proposed that the seismic response analysis of the base-isolated structure under the action of near fault pulse-like earthquake, the site of the structure and the focal mechanism of the ground motion should be considered. Bai et al.³ carried out the nonlinear dynamic analysis of the structure under rare earthquake, it was found that the near-fault pulse-like ground motion caused greater seismic responses to the structure than no pulse-like earthquake, and the response is significantly concentrated in the time of velocity pulse. Yan et al.⁴ discussed the

influence of long-period velocity pulse of near fault earthquake on structure dynamic response, and obtained that the dynamic response of base-isolated structure under near-fault earthquake action was obviously larger than that under far-field earthquake action.

Historical experience has proven that large storage tanks are very vulnerable in the face of natural disasters such as earthquakes. Earthquakes will not only cause damage to the tanks themselves, but also cause catastrophic consequences such as explosion, fire, and environmental pollution. The losses caused by these damages far exceed the economic value of the tanks themselves and liquid. Compared with the far-field earthquake, many near-field earthquakes contain single or multiple velocity pulses, which may make the structure subject to large energy impact in a very short time, resulting in serious damage to the structure. It is necessary to consider the liquid-solid coupling effect in the study of dynamic response of liquid storage tank under earthquake. Housner⁵ and Haroun⁶ proposed the classical two-particle and three-particle spring-mass model to simulate the fluid-solid coupling. Ge et al.⁷ proposed a nonlinear

simple pendulum system model suitable for simplified calculation of liquid storage tank. Kildashti et al.⁸ used the added mass method to simulate the fluid-structure interaction, and obtained that the foundation elasticity would lead to a lower critical earthquake intensity. Columbo and Almazán⁹ proposed a simplified nonlinear model to estimate the rolling resistance and stress distribution of the floor. Rawat et al.¹⁰ used sound-structure and Euler-Lagrange coupling methods to analyze the liquid storage tank. Based on the potential flow theory and appropriate boundary conditions, Lv et al.¹¹ derived the analytical solution of seismic response calculation. Bakalis and Karamanos¹² studied the uplift mechanism of no anchored storage tank under strong lateral load by using three-dimensional finite element model. Although the simplified model based on Haroun-Housner model can accurately calculate the base shear force and overturning moment, it can not obtain the stress distribution of the tank wall, the uplift of the tank bottom and the buckling failure of the tank wall. Therefore, it is very necessary to use the three-dimensional calculation model to study the seismic response of the tank.

With the rapid development of petrochemical industry, the earthquake prevention and disaster reduction of liquid storage tank has become an important research topic. Shock absorption control opens up a new way for the seismic design of liquid storage tank. Safari and Tarinjad¹³ studied the seismic response of the base-isolated liquid storage tank by using the frequency domain random method, and obtained that the sliding bearing can significantly reduce the sloshing response. Compagnoni et al.¹⁴ studied the seismic performance of the isolated tank with sliding concave support, and found that it could reduce the base shear, but had no significant effect on the sloshing displacement. Cheng et al.¹⁵ carried out the shaking table test of sliding isolation liquid storage structure, and obtained that sliding isolation had significant control effect on structure dynamic response and liquid sloshing. Nikoomanesh et al.¹⁶ proposed a vertical isolation system for liquid storage tanks, and the parameter research showed that the system was more effective for slender liquid storage tanks. Kim et al.¹⁷ established a set of optimal friction material selection system for friction pendulum isolation tank, and obtained a lower friction coefficient through vulnerability analysis, which was more helpful to prevent tank damage. Jiang et al.¹⁸ put forward the optimization design method of the tank with inertial vessel isolation system, and obtained that the method could meet the requirements of sloshing wave height and effectively reduce the base shear force and the displacement of isolation layer. Lv et al.¹⁹ deduced a simplified mechanical model of variable curvature rolling isolation tank considering liquid sloshing, and obtained that this kind of isolation had shock absorption effect on base shear, overturning moment and liquid sloshing. Zhou et al.²⁰ studied the dynamic response of the tank with anchorage and replacement of damper through shaking table test and finite element method, and obtained that the new tank could realize the recovery function by replacing the damper after the earthquake. Krishnamoorthy²¹ used the finite element method to simulate the fluid storage tank with friction pendulum, and pointed out that the finite element method considering fluid structure coupling was more suitable for the analysis of FPS liquid storage tank. In general, although researchers have

carried out a series of researches on rubber isolation, friction pendulum isolation, vertical isolation, inertial container isolation and rolling isolation liquid storage tank, there are few researches on damper shock absorption. Rubber isolation can reduce the dynamic response of the tank itself, but it has little control effect on the sloshing wave height, and even has amplification effect. In contrast, some new isolation measures have good shock absorption effect on the dynamic response and liquid sloshing of the tank.

To sum up, the near fault earthquake is likely to have more adverse effects on the structure, and the liquid-solid coupling effect under the earthquake will make the liquid tank in a more complex stress state. Therefore, it is of great significance to carry out the research on the dynamic response law of the liquid tank under the near-fault earthquake and put forward the economic and applicable seismic isolation method. The three-dimensional numerical calculation models of no isolation and sliding isolation liquid storage tank are established. Twelve near fault seismic waves with different focal mechanisms are selected from PEER. The variation of seismic response of liquid storage tank during PGA increasing is studied. The seismic responses of liquid storage tank under near-fault earthquake with different focal mechanisms is compared and analyzed. This paper discusses the effectiveness of the sliding isolation limiting device on the shock absorption control of the liquid storage tank, and finally analyzes the influence of the limiting device on the seismic response, so as to provide reference for the engineering application and earthquake prevention and disaster reduction of the liquid storage tank.

2. FUNDAMENTAL THEORY

2.1. Boundary Conditions and Initial Conditions

$\Phi(r, \theta, t)$ was used to represent the velocity potential function of liquid, which should satisfy the Laplace equation, i.e:

$$\frac{\partial^2 \Phi}{\partial r^2} + \frac{1}{r} \frac{\partial \Phi}{\partial r} + \frac{1}{r^2} \frac{\partial^2 \Phi}{\partial \theta^2} + \frac{\partial^2 \Phi}{\partial z^2} = 0. \quad (1)$$

There are three kinds of typical boundary conditions for a liquid storage tank under earthquake action, namely, wall plate Γ_w , bottom plate Γ_b and free surface Γ_f . On the free surface Γ_f , dynamic and motion conditions need to be satisfied. The boundary conditions and initial conditions that velocity potential function needs to satisfy were as follows:

$$\left\{ \begin{array}{l} \frac{\partial \Phi(r, \theta, t)}{\partial z} \Big|_{z=0} = 0, \quad \Gamma_b \\ \frac{\partial \Phi(r, \theta, t)}{\partial r} \Big|_{r=R} = (\dot{s}(z, t) + \dot{u}_g(t)) \cos \theta, \quad \Gamma_w \\ \frac{\partial \Phi(r, \theta, t)}{\partial \theta} \Big|_{\theta=0, \pi} = 0, \quad \Gamma_w \\ \frac{\partial \Phi(r, \theta, t)}{\partial t} \Big|_{z=h_w} + gf = 0, \quad \Gamma_f \\ \Phi|_{t=0} = \phi_0, \quad \dot{\Phi} \Big|_{t=0} = \dot{\Phi}_0 \end{array} \right. ; \quad (2)$$

where g was the acceleration of gravity, f was the wave equation of free surface, h_w was the height of liquid surface, t was the time, s was the elastic deformation of tank wall.

When the liquid interacts with solid medium, equilibrium and compatibility equations must be satisfied on the contact

surface:

$$\begin{cases} \tau^s \cdot n = \tau^f \cdot n \\ u_s^I = u_f^I \\ v_s^I = v_f^I = \bar{v}_f^I \\ a_s^I = a_f^I = \bar{a}_f^I \end{cases} ; \quad (3)$$

where n was the normal vector on the contact surface; u_s and u_f were the structure and liquid displacements on the contact surface; v_s , v_f and \bar{v}_f were the structure, liquid and coordinate system velocities; a_s , a_f and \bar{a}_f were the structure, liquid and coordinate system accelerations; I represented the contact surface.

2.2. Liquid Solid Coupling Dynamic Equation

The fluid structure interaction was realized by pressure vector \mathbf{p} and coefficient matrix \mathbf{B} , and the liquid solid coupling dynamic equation is:²²

$$\begin{bmatrix} M_s & 0 \\ \rho_f B & E \\ K_s & -B^T \\ 0 & H \end{bmatrix} \begin{bmatrix} \dot{r} \\ \dot{p} \\ r \\ p \end{bmatrix} + \begin{bmatrix} C_s & 0 \\ 0 & A \end{bmatrix} \begin{bmatrix} \dot{r} \\ \dot{p} \end{bmatrix} + \begin{bmatrix} -M_s \ddot{u}_g \\ -q_0 \end{bmatrix} ; \quad (4)$$

where \mathbf{M}_s , \mathbf{C}_s and \mathbf{K}_s were the structure mass, damping and stiffness matrices, respectively, \mathbf{r} was the displacement vector, \ddot{u}_g was the seismic acceleration vector, ρ_f was the density of liquid, \mathbf{p} was the liquid pressure vector, q_0 was the input excitation vector transferred from the structure to the liquid, \mathbf{H} , \mathbf{A} , \mathbf{E} and \mathbf{B} are coefficient matrices.

3. NUMERICAL EXAMPLE

3.1. Calculation Model

The diameter of the tank was 10m, the height was 10m, the liquid storage height was 8m, and the thickness of the wall plate was 20mm. The sliding isolation design was adopted, and a total of 8 limiting devices were set at the bottom of the tank. Assuming that the liquid storage tank was a bilinear elastic-plastic model, the tank wall elastic modulus was 2×10^{11} Pa, the Poisson's ratio was 0.3, and the density was 7850kg/m^3 , the shell element is used to simulate the liquid storage tank plate. Beam element was adopted for the limiting device, and bilinear elastic-plastic model was adopted for the material. The specific material parameters are shown in Table 1 [23-24]. Potential fluid model was used for the liquid with density of 1000kg/m^3 and bulk modulus of 2.3×10^9 Pa. The contact surface is used to simulate the mechanical behavior of sliding isolation bearing. Considering the fluid solid coupling effect, the three-dimensional numerical calculation models of no isolation and isolation liquid storage tank are established, as shown in Fig. 1.

3.2. Earthquake Waves

Based on the strong motion database of PEER, 12 near field seismic records with different focal mechanisms were selected, among which 3 were Reverse, Strike slip, Reverse Oblique and Normal focal mechanisms. The criteria for selecting near field seismic records were as follows: the fault distance was not

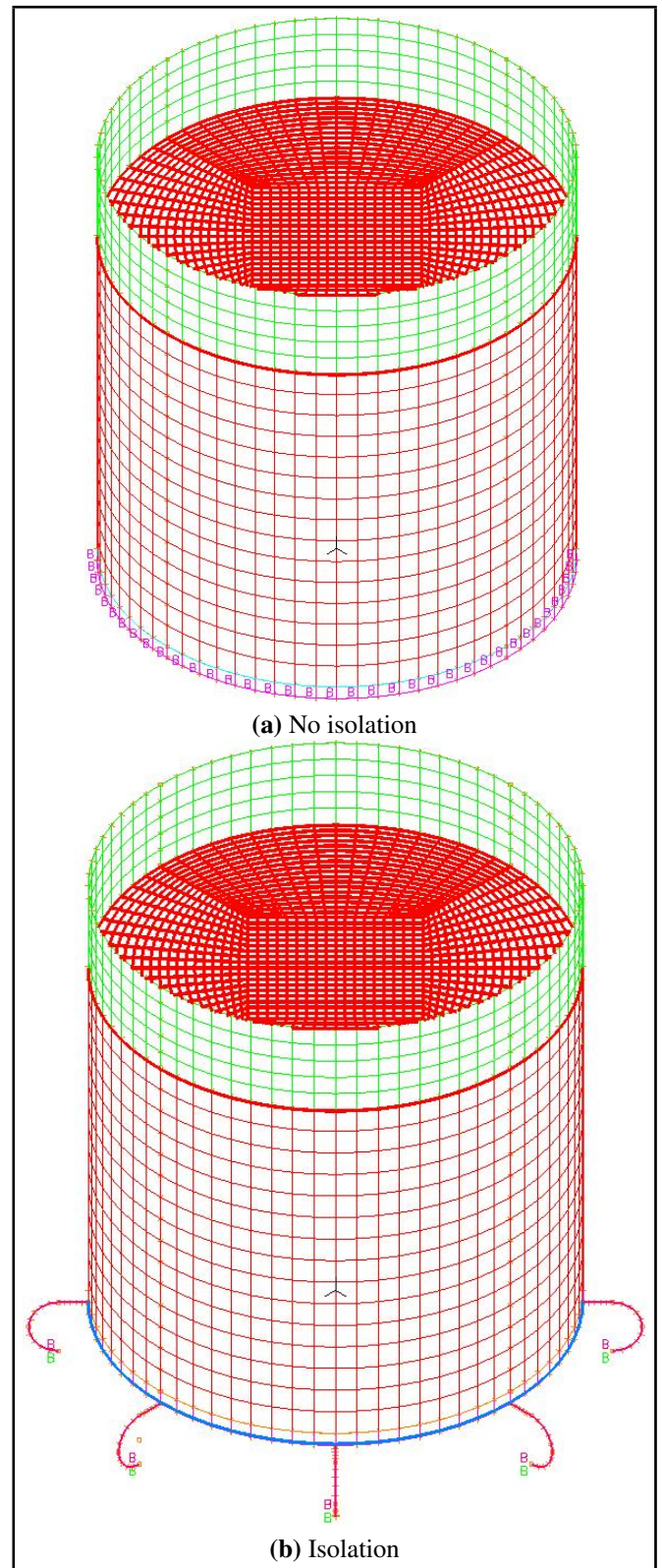


Figure 1. Calculation model.

more than 20km, the ratio of peak ground velocity (PGV) to peak ground acceleration (PGA) was greater than 0.2, and the moment magnitude was greater than 6.0. The detailed information of seismic waves is shown in Table 2. Fig. 2 shows the acceleration response spectrum and average acceleration response spectrum of near-fault earthquakes.

It can be seen from Fig. 2 that the average value of seismic acceleration response spectrum of N-type focal mecha-

Table 1. Material parameters of bilinear elastic-plastic model.

Elastic modulus (Pa)	Poisson's ratio	Yield strength (MPa)	Density (kg/m ³)	Strain hardening modulus (Pa)	Yield strain	Maximum plastic strain
2×10^{11}	0.3	235	7800	2×10^9	0.001	0.02

Table 2. Seismic wave information.

Earthquake name	Station name	Mechanism	Magnitude	Rrup (km)	Tp-Pulse (s)
L'Aquila_ Italy	L'Aquila - Parking	Normal (N)	6.3	5.38	1.981
L'Aquila_ Italy	L'Aquila - V. Aterno - Centro Valle		6.3	6.27	1.071
L'Aquila_ Italy	L'Aquila - V. Aterno -F. Aterno		6.3	6.55	1.176
Chi-Chi_ Taiwan	CHY101	Reverse Oblique (RO)	7.62	9.94	5.341
Chi-Chi_ Taiwan	TCU049		7.62	3.76	10.22
Chi-Chi_ Taiwan	TCU068		7.62	0.32	12.285
Montenegro_ Yugoslavia	Bar-Skupstina Opstine	Reverse (R)	7.10	6.98	1.442
Cape Mendocino	Bunker Hill FAA		7.01	12.24	5.362
Cape Mendocino	Centerville Beach_ Naval Fac		7.01	18.31	1.967
Kocaeli_ Turkey	Arcelik	Strike Slip (SS)	7.51	2.19	5.124
Darfield_ New Zealand	DSLCL		7.00	8.46	7.826
Kocaeli_ Turkey	Gebze		7.51	10.92	5.992

nism was obviously larger than that of other three types of focal mechanisms, and the order was $N > RO > SS > R$. It can be seen from Fig. 3 the velocity pulses of near fault pulse-like earthquakes with different focal mechanisms were very different, such as velocity pulse amplitude and number of velocity pulses.

3.3. Seismic Responses

Liquid sloshing wave height, wall displacement, liquid pressure and wall effective stress were selected as the analysis objects. The dynamic responses of liquid storage tanks under different focal mechanisms were compared, and the influence of focal mechanisms on seismic responses was analyzed. With the increase of earthquake intensity, the variation of seismic response is discussed. The specific calculation results are shown in Figs. 4,5, 6, 7, 8.

It can be seen from Fig. 4 that under the action of seismic waves of different focal mechanisms, the difference of liquid sloshing wave height was larger, the liquid sloshing wave height corresponding to N-type focal mechanism was smaller, and the liquid sloshing wave height of L'Aquila - V. Aterno -F. Aterno earthquake was the smallest, the sloshing wave height corresponding to RO-type focal mechanism was larger, and the liquid sloshing wave height of CHY101 earthquake is the largest. The liquid sloshing wave height increased with the increase of PGA. When PGA was 0.4 g, the maximum liquid sloshing wave height under CHY101 earthquake was about 2.5 m. Excessive liquid sloshing wave height caused the failure of the liquid storage tank, and liquid overflow also caused secondary disasters such as environmental pollution.

It can be seen from Fig. 5 that the displacement of the tank wall varied greatly under the action of seismic waves of different focal mechanisms. The displacement of the tank wall corresponding to the N-type focal mechanism was larger, and the displacement of the tank wall under the action of L'Aquila - V. Aterno -F. Aterno earthquake was the largest. When the PGA was 0.4 g, the displacement of the wall plate reached 10.25 mm, and the displacement of the tank wall under the R-type source mechanism was smaller.

It can be seen from Fig. 6 that under the action of seismic waves of different focal mechanisms, the difference of liquid

pressure is large, and the corresponding liquid pressure of the N-type focal mechanism was large, and the liquid pressure under the L'Aquila - V. Aterno -F. Aterno earthquake was the largest. When the PGA was 0.4 g, the maximum liquid pressure reaches 465.90 kPa, and the difference of liquid pressure under other three types of focal mechanisms was small, under the action of R-type focal mechanism seismic wave, the liquid pressure changed gently.

It can be seen from Fig. 7 that under the action of seismic waves of different focal mechanisms, the effective stress of tank wall was quite different, the effective stress of tank wall corresponding to the N-type focal mechanism was relatively large, and the effective stress of tank wall under the L'Aquila - V. Aterno -F. Aterno earthquake was the largest. When the PGA was 0.4 g, the maximum effective stress of the tank wall reached 136.39 MPa, and the difference of effective stress of tank wall under the other three types of focal mechanisms was relatively small. Based on the calculation of the above 12 seismic waves, the average values of liquid sloshing wave height, wall plate displacement, liquid pressure and wall plate effective stress under the action of four types of focal mechanism earthquakes are drawn in Fig. 7, and the influence of focal mechanism on the seismic response of liquid storage tank is further analyzed.

It can be seen from Fig. 8 that for the liquid sloshing wave height, the RO-type focal mechanism corresponds to the largest one. The order of liquid sloshing wave height under the action of seismic waves of four types of focal mechanisms was $RO > R > SS > N$. For the displacement of tank wall, liquid pressure and effective stress, except for the case of 0.1g, the value under the N-type focal mechanism was obviously larger than that of the other three types of focal mechanisms. Moreover, the displacement, liquid pressure and effective stress of the tank wall have little difference under RO-type, R-type and SS-type focal mechanism earthquakes.

3.4. Study on the Shock Absorption Performance

Based on the above analysis, the dynamic response recorded by L'Aquila-V.Aterno-F.Aterno was larger. Limited to space, only taking the L'Aquila-V.Aterno-F.Aterno record as an ex-

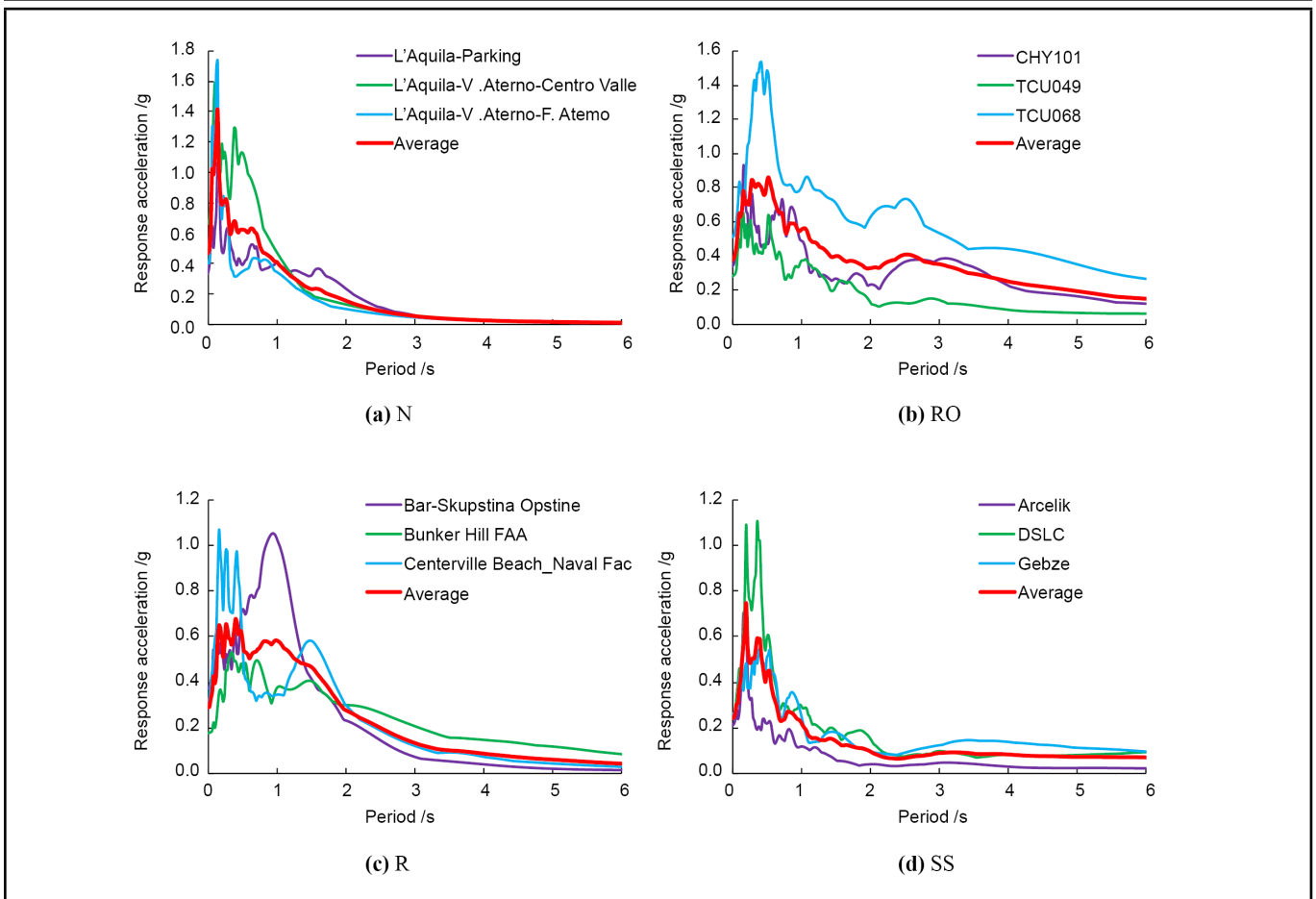


Figure 2. Acceleration response spectrum.

ample, the PGA was adjusted to 0.62 g, the friction coefficient was set to 0.02, and the diameter of limiting device was set to 20 mm. The seismic response of without isolation and sliding isolation limiting liquid storage tank was compared, and the effectiveness of shock absorption control measures for near fault seismic response control was discussed. The calculation results of the maximum sloshing wave height, the maximum effective stress of the wall plate and the maximum liquid pressure of the liquid storage tank are shown in Figs. 9, 10, 11.

It can be seen from Figs. 9, 10, 11 that when the PGA was 0.62 g, the wall effective stress of no isolation liquid storage tank was 174.700 MPa. After sliding isolation, the effective stress of the wall plate was reduced to 67.610 MPa, which is far less than the yield strength of the steel. The sloshing wave height was reduced from 0.481 m to 0.424 m. The sliding isolation also plays a certain role in controlling the sloshing wave height. The reason for the smaller shock absorption effect may be due to the influence of the limiting device. The liquid pressure of the without isolated liquid tank is 4773.686 kPa, which is reduced to 214.094 kPa after sliding isolation. Sliding isolation has a very significant shock absorption effect on the liquid storage tank, which helps to ensure the safety of the liquid storage tank under near fault strong earthquake.

3.5. Influence of Limiting Device

The diameter of the limiting device was one of the important design parameters, which not only affected the dynamic

response of the system, but also affects the natural vibration characteristics of the system. The advantage of the limiting device was that it solved the displacement overrun problem of the isolation layer. Its disadvantage was equivalent to increasing the stiffness of the isolation layer, which will affect the shock absorption effect of the isolation. Therefore, it was necessary to explore the influence law of the diameter of the limiting device on the seismic response. Taking the L'Aquila-V.Aterno-F.Aterno seismic record as an example, the influences of the diameter of the limiting device on the seismic responses are shown in Fig. 12.

From Fig. 12, the influence of the limiting device diameter on the effective stress and the wave height of liquid sloshing is very significant, and the influence on the liquid pressure is relatively small. When the diameter of the limiting device is 24 mm, the liquid sloshing wave height reaches the minimum value. When the diameter of the limiting device reaches 36 mm, the corresponding liquid sloshing wave height of the isolation device is larger than that of without isolation. When the diameter of the limiting device is 20 mm, the effective stress of the tank wall is relatively large. When the diameter of the limiting device is 24 mm and 32 mm, the effective stress of the tank wall reaches a smaller value, and the sliding isolation has a better effect on shock absorption. With the increase of the diameter of the limiting device, the liquid pressure changes very little.

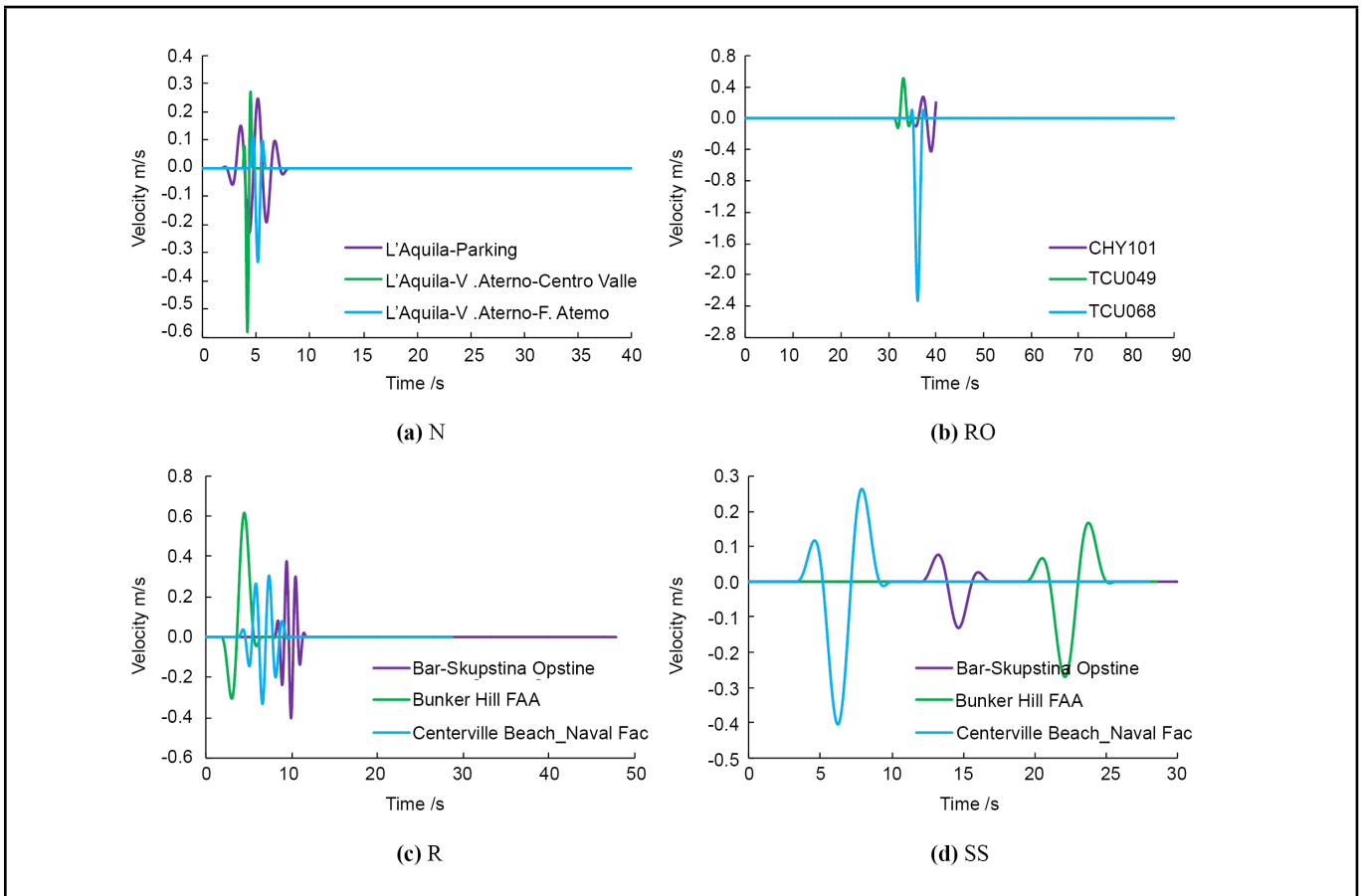


Figure 3. Velocity pulses.

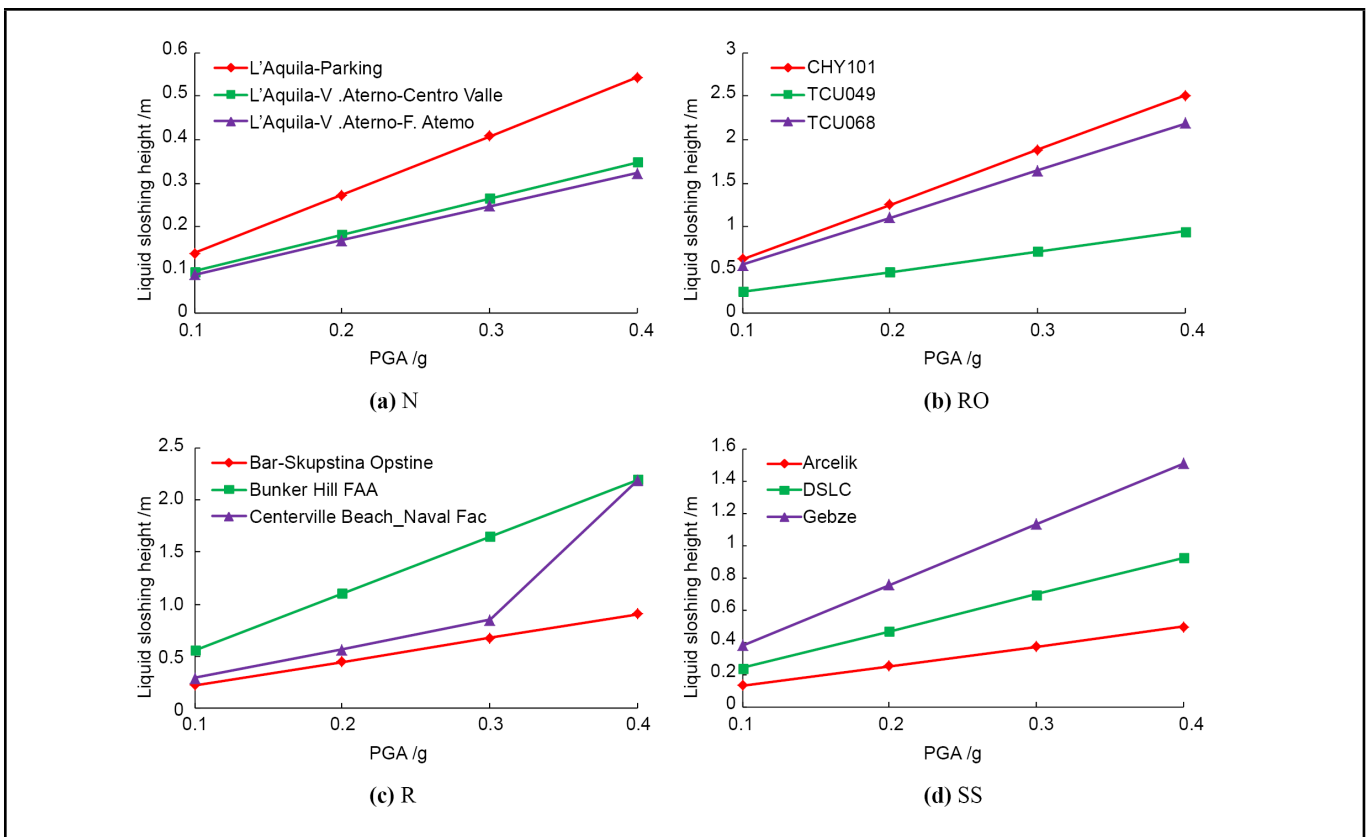


Figure 4. Wave height.

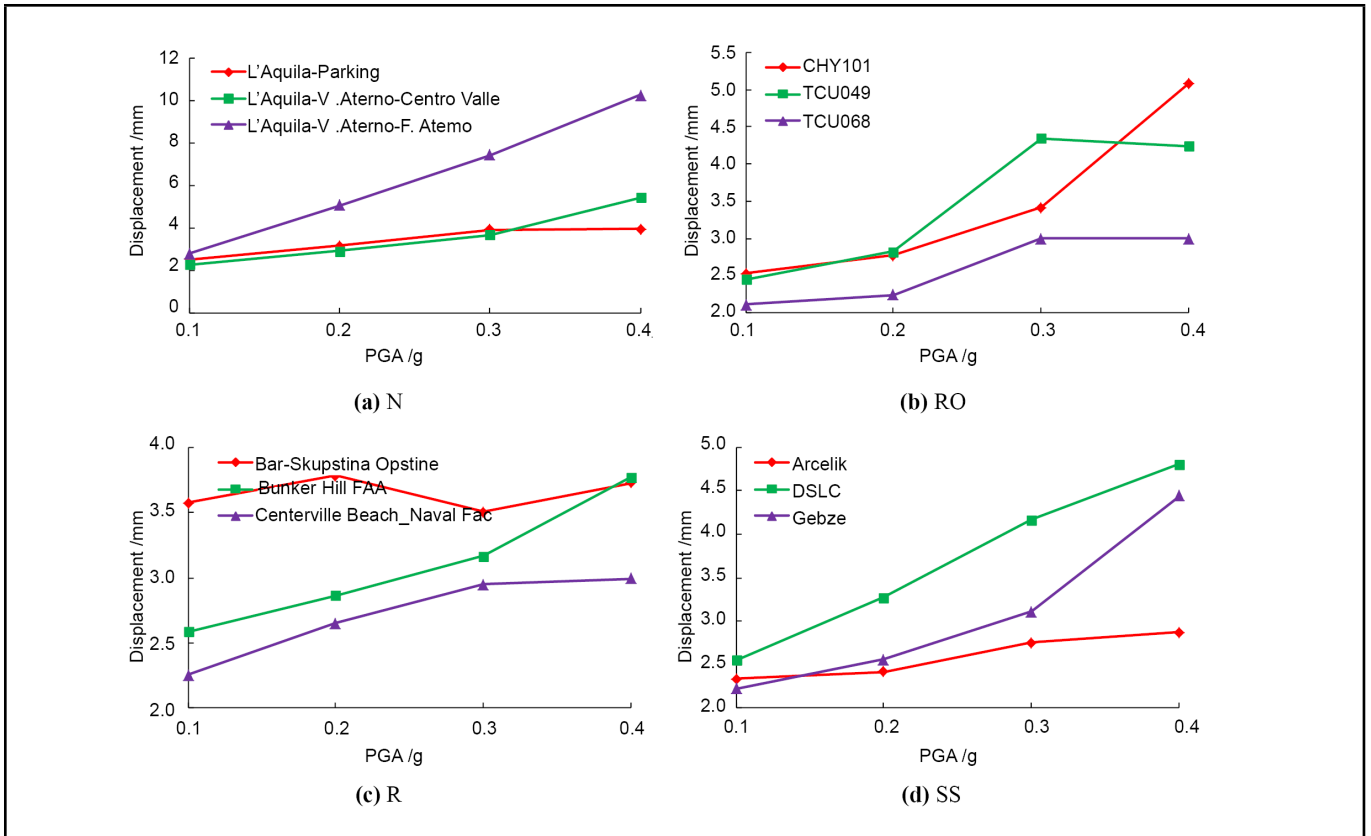


Figure 5. Wall displacement.

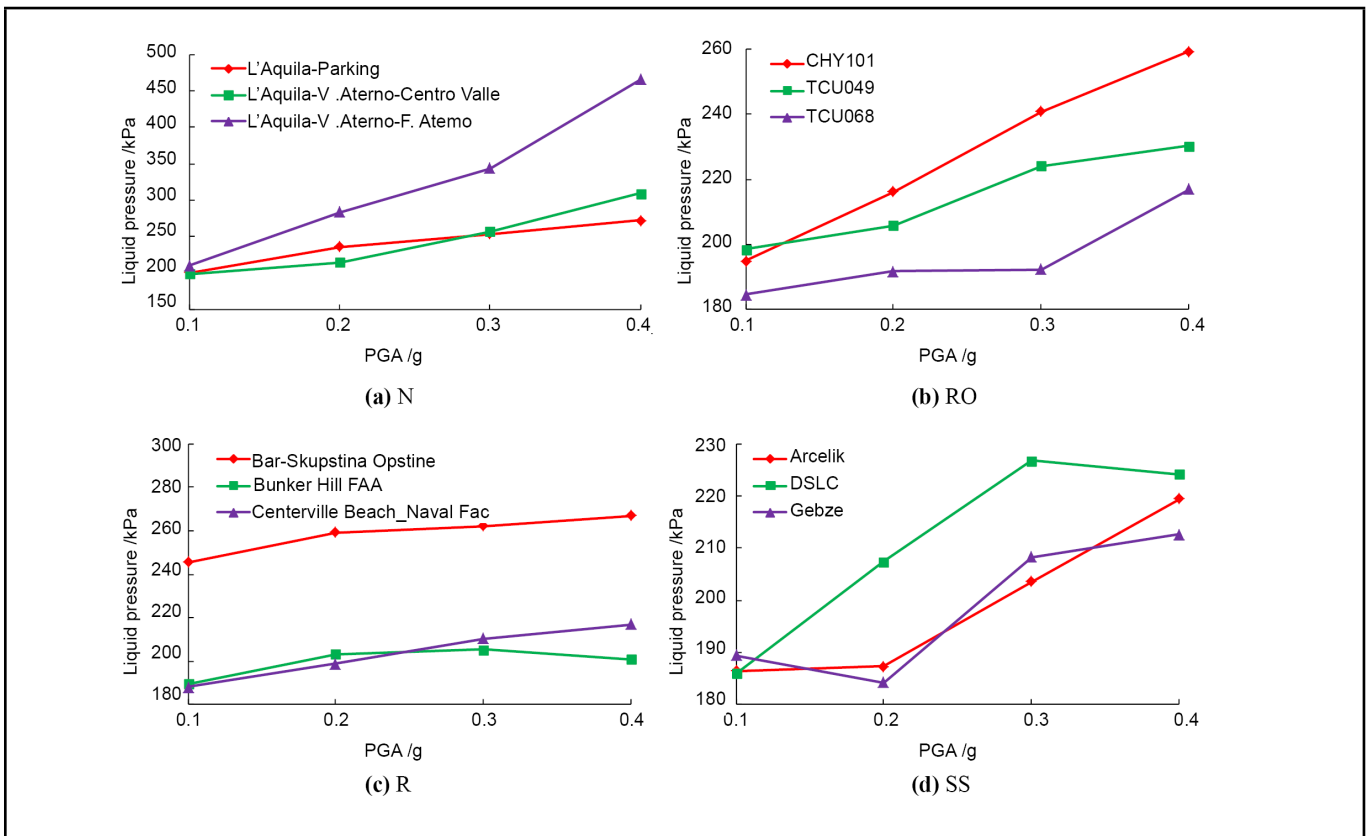


Figure 6. Liquid pressure.

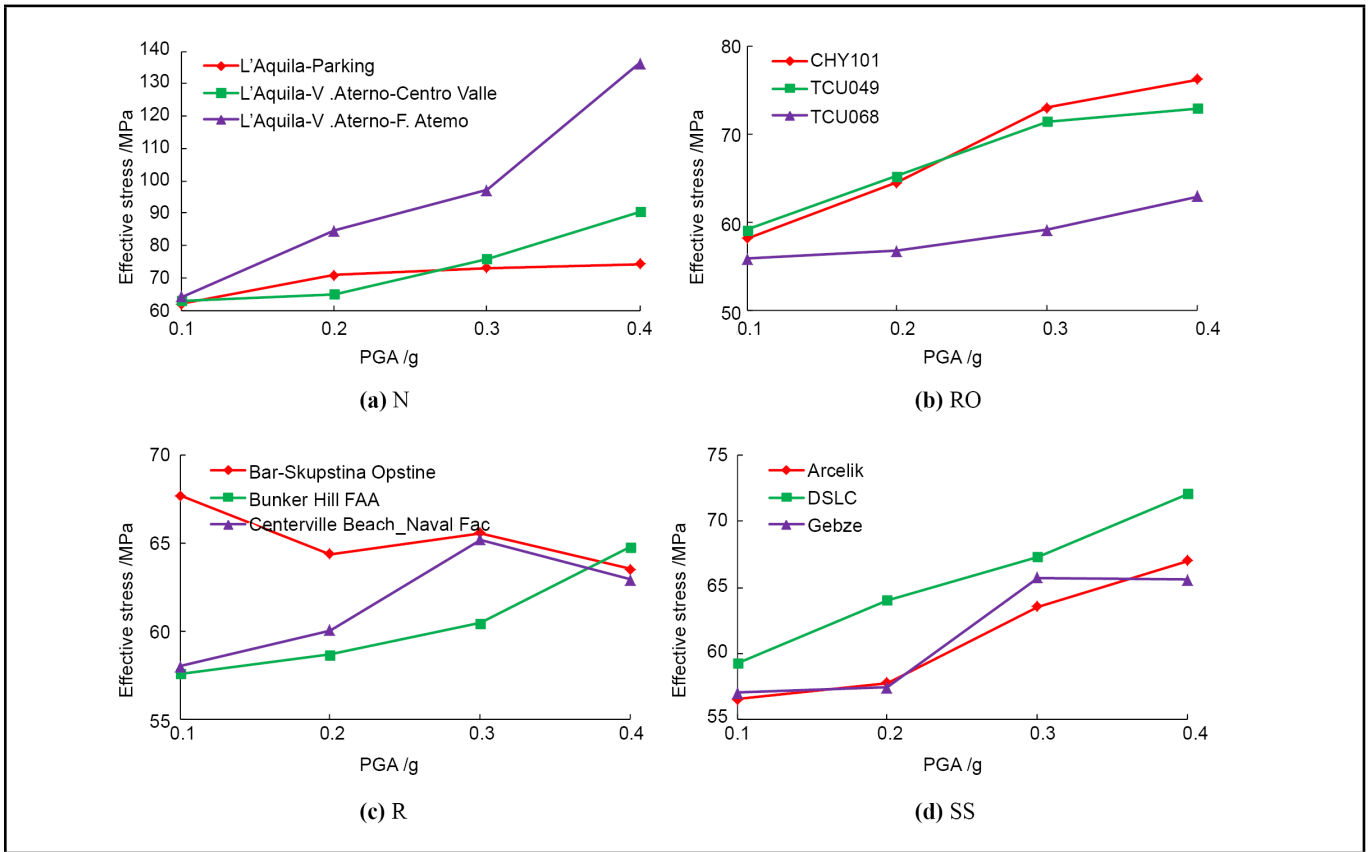


Figure 7. Wall effective stress.

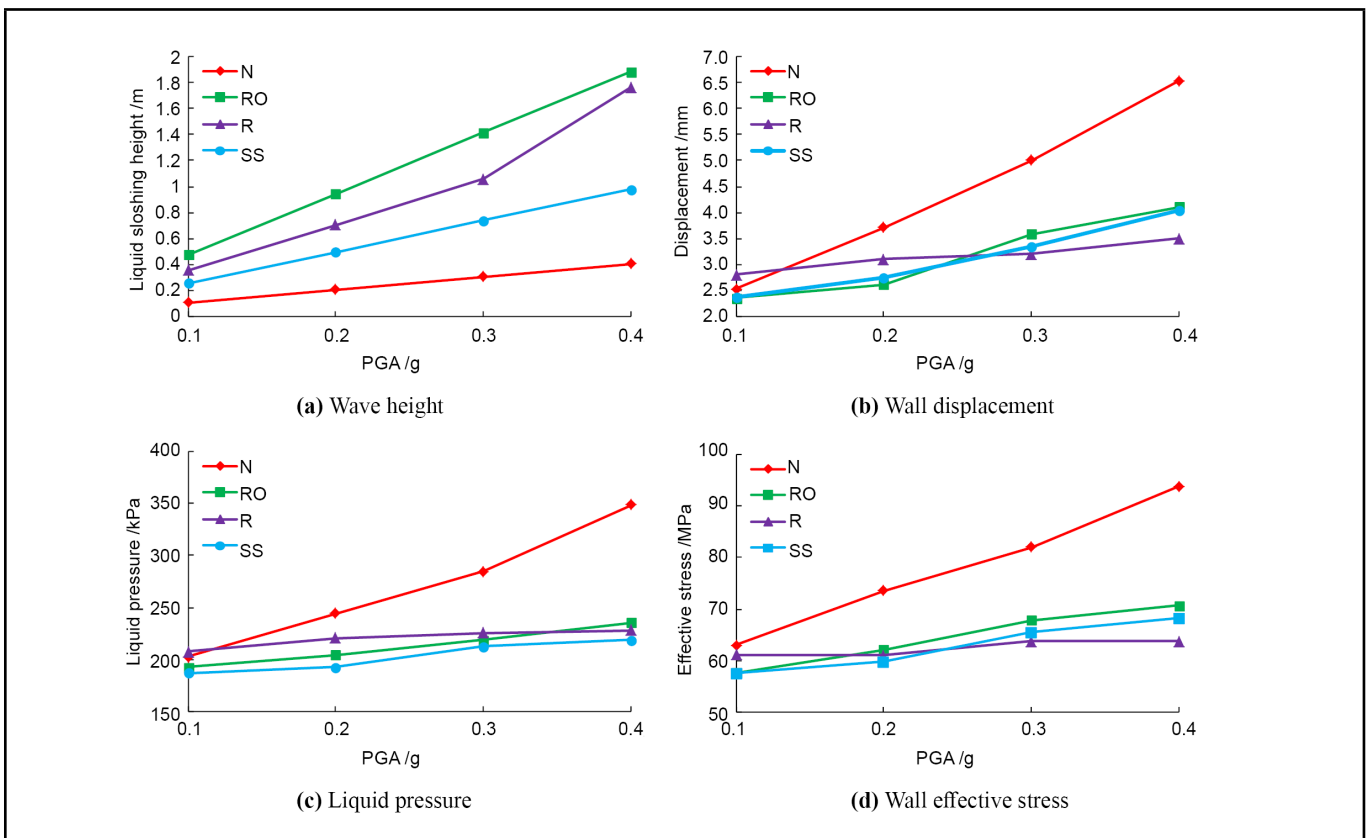


Figure 8. Dynamic response corresponding to four types of focal mechanism earthquakes.

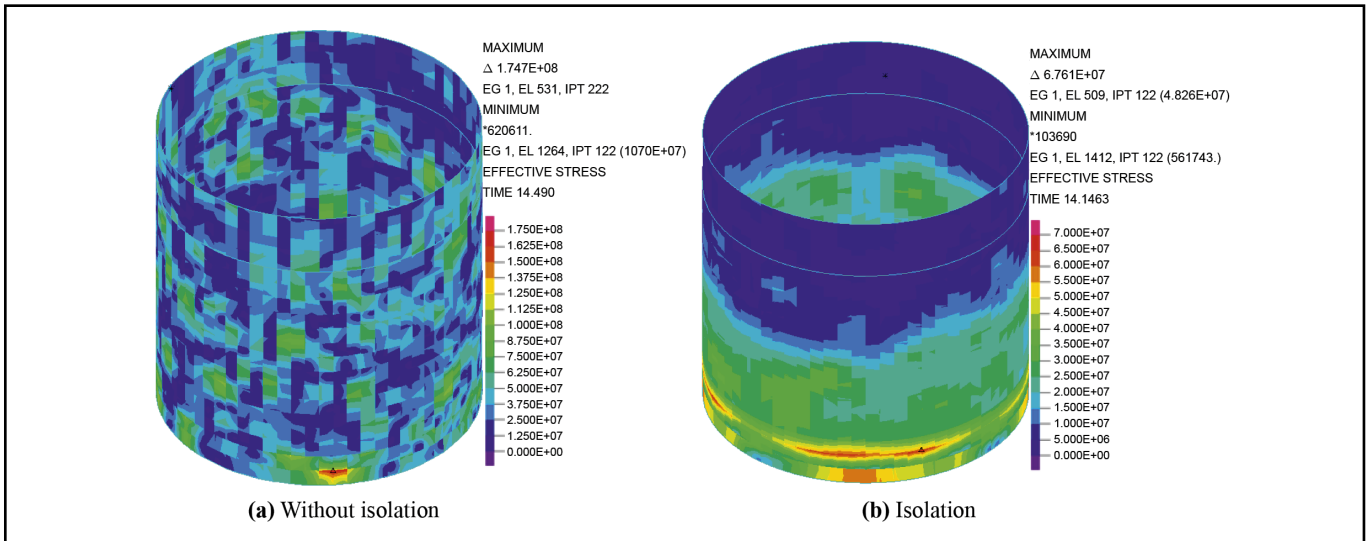


Figure 9. Effective stress of wall plate under L'Aquila-V.Aterno-F.Aterno earthquake.

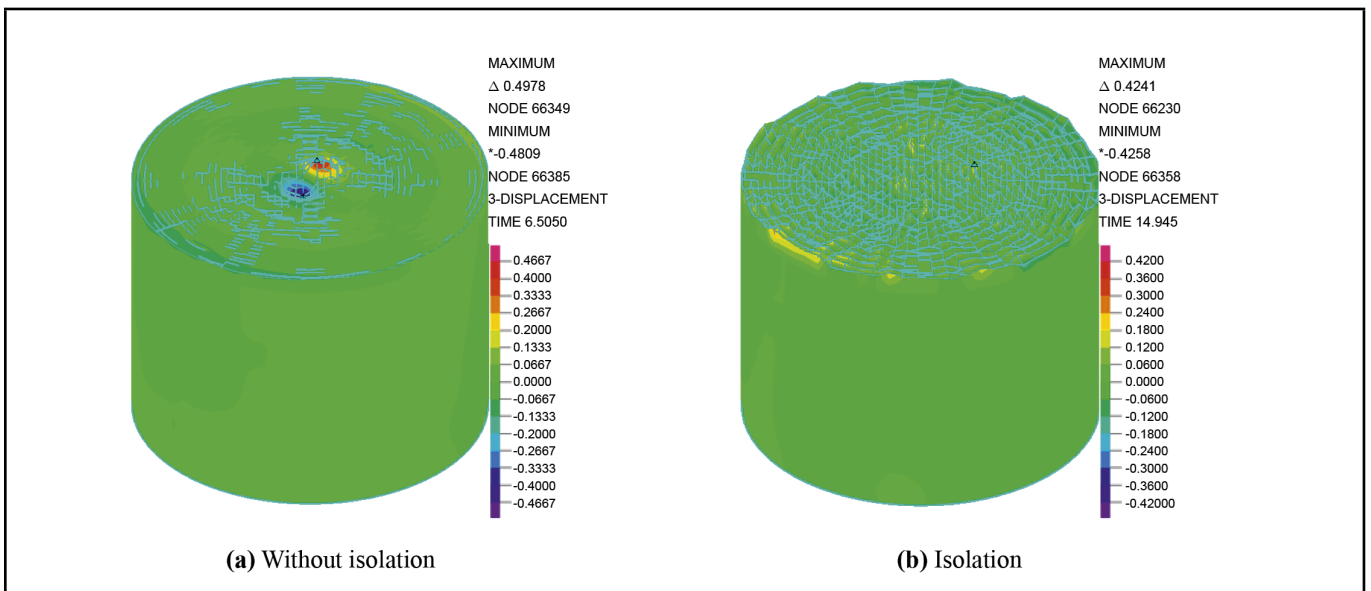


Figure 10. Liquid sloshing wave height under L'Aquila-V.Aterno-F.Aterno earthquake.

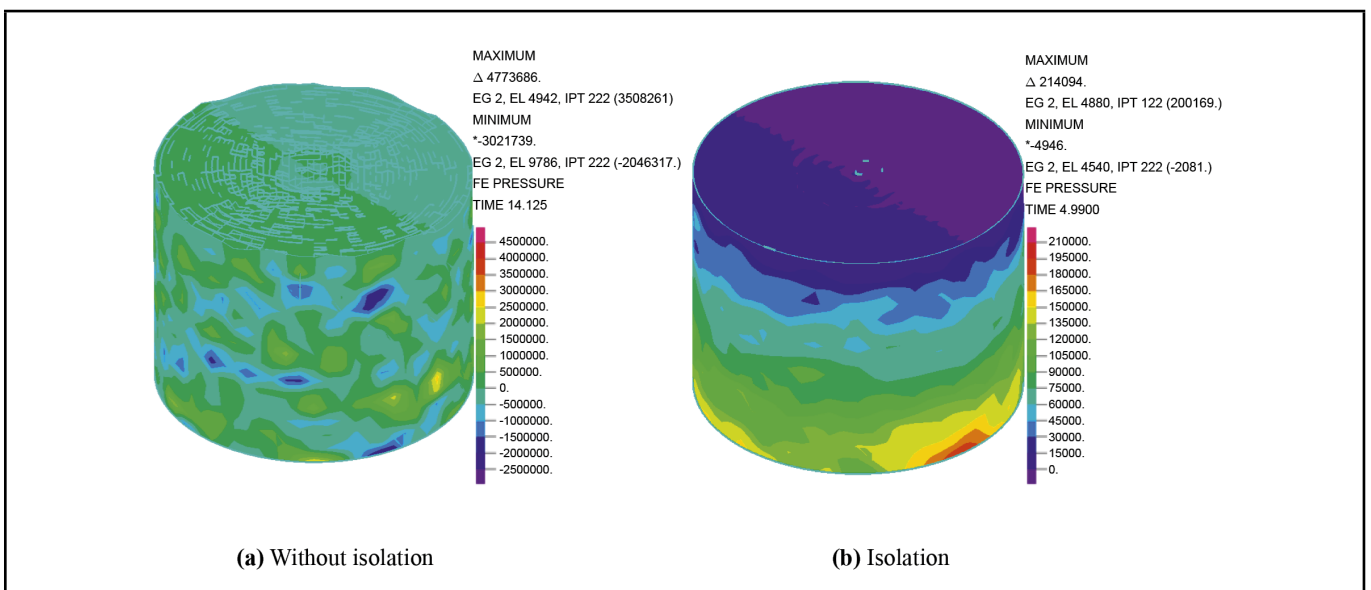


Figure 11. Liquid pressure under L'Aquila-V.Aterno-F.Aterno earthquake.

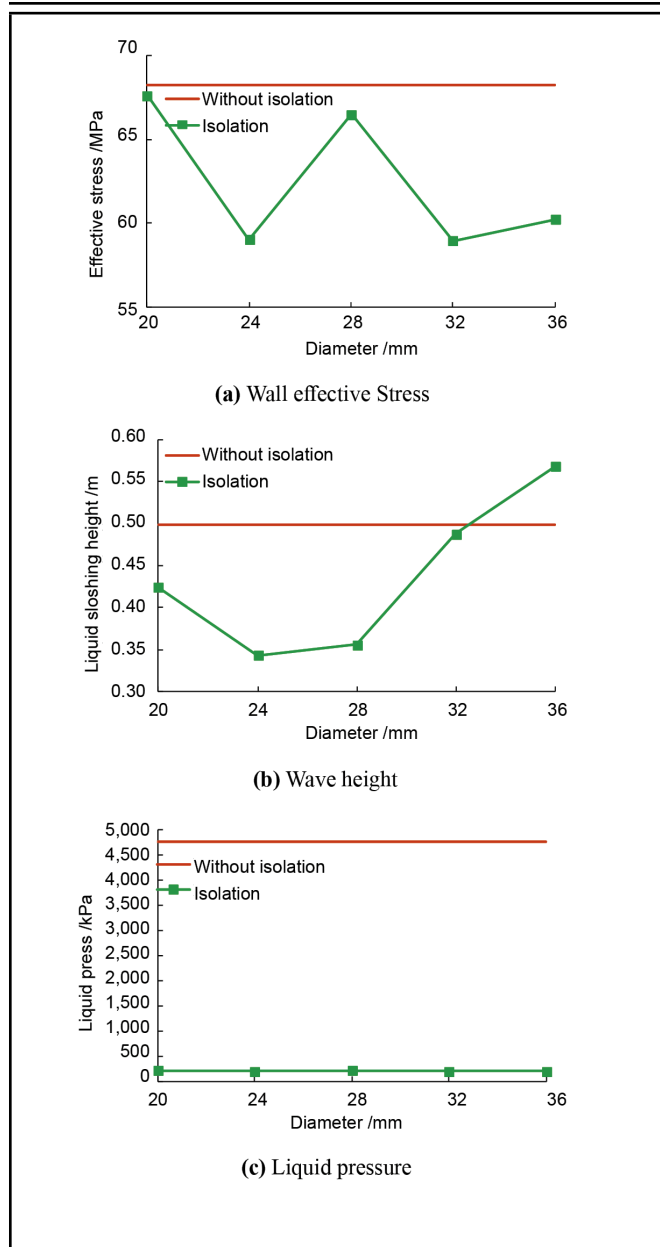


Figure 12. Influence of diameter of limiting device on dynamic response under L'Aquila-V.Aterno-F.Aterno earthquake.

4. CONCLUSION

The three-dimensional numerical model of non-isolated and isolated liquid storage tank is established. The seismic responses of non-isolated liquid storage tank under different source mechanism are studied. The effectiveness of sliding isolation for dynamic response control under near-fault earthquake is discussed. The main conclusions are as follows:

1. For the non-isolated liquid storage tank, the liquid sloshing wave height under RO-type focal mechanism earthquake is the largest, especially the liquid sloshing wave height under CHY101 earthquake record is about 2.5 m. The order of liquid sloshing wave height under four types of focal mechanism earthquake is $RO > R > SS > N$. For the displacement, liquid pressure and effective stress of the tank wall, the response of the N-type focal mechanism is obviously larger than that of the other three types of focal mechanisms.

2. When PGA is 0.62 g, the wall effective stress of non-isolated liquid storage tank is 174.700 MPa. After sliding isolation, the effective stress and liquid pressure of the tank wall are significantly reduced, and the liquid sloshing wave height is controlled to a certain extent.
3. When the diameter of the limiting device is 24 mm, the liquid sloshing wave height, effective stress and liquid pressure are relatively small.
4. Sliding isolation limiting control system can achieve good shock absorption effect, low cost and simple construction, which has a very good application prospect in the earthquake prevention and disaster reduction of liquid storage tank.

CONFLICTS OF INTEREST

The authors declare that they have no conflicts of interest regarding the publication of this paper.

ACKNOWLEDGMENTS

This paper is a part of the Scientific Research Fund of Institute of Engineering Mechanics, China Earthquake Administration (Grant No. 2020D26), a part of the National Natural Science Foundation of China (Grant No. 51908267, 52168071), a part of the Gansu Youth Science and Technology Fund Plan (Grant No. 20JR5RA433), a part of the Ningxia Natural Science Fund Project (Grant No. 2020AAC02007), and a part of the Hongliu Outstanding Young Talents Support Program of Lanzhou University of Technology (Grant No. 04-061807).

REFERENCES

- ¹ Pan, Q. F., Yan, G. Y., Ying-Xiong, W. U., & Fang, Y. W. (2019). Seismic absorption performance of composite isolation for high-rise buildings subjected to near-fault pulse ground motions, *Journal of Vibration Engineering*, **32**(5), 111–121. <https://doi.org/10.16385/j.cnki.issn.1004-4523.2019.05.013>
- ² Du, Y., Xu, T., & Hong, N. (2017). Spectrum and intensity indices of near-fault ground motions based on different focal mechanisms, *China Civil Engineering Journal*, **5**(5), 81–87. <https://doi.org/10.15951/j.tmgcxb.2017.05.009>
- ³ Bai, J., Cheng, F., Jin, S., Pan, Y., & Zhao, J. (2018). Seismic performance of PC frame structures with buckling-restrained brace subjected to near-fault pulse-like ground motions, *Journal of Building Structure*, **39**(S1), 110–117. <https://doi.org/10.14006/j.jzjgxb.2018.S1.014>
- ⁴ Yan, G. Y., Xiao, X. F., Wu, Y. X., & Fang, Y. W. (2018). Shaking table test of isolated single-tower structures with a large chassis under near-fault ground motions, *Journal of Vibration Engineering*, **31**(05), 799–810. <https://doi.org/10.16385/j.cnki.issn.1004-4523.2018.05.009>

- ⁵ Housner, G. W. (1957). Dynamic pressure on accelerated fluid container. *Bulletin of the Seismological Society of America*, **47**(1), 15–35. <https://doi.org/10.1785/BSSA0470010015>
- ⁶ Haroun, M. A. (1983). Vibration studies and tests of liquid storage tanks. *Earthquake Engineering and Structural Dynamics*, **11**(2), 179–206. <https://doi.org/10.1002/eqe.4290110204>
- ⁷ Ge, Q. Z., Weng, D. G., & Zhang, R. F. (2014). A nonlinear simplified model of liquid storage tank and primary resonance analysis, *Engineering Mechanics*, **31**(5), 166–171. <https://doi.org/10.6052/j.issn.1000-4750.2012.12.0944>
- ⁸ Kildashti, K., Mirzadeh, N., & Samali, B. (2018). Seismic vulnerability assessment of a case study anchored liquid storage tank by considering fixed and flexible base restraints, *Thin-Walled Structures*, **123**, 382–394. <https://doi.org/10.1016/j.tws.2017.11.041>
- ⁹ Colombo, J. I., & Almazán, J. L. (2019). Simplified 3D model for the uplift analysis of liquid storage tanks, *Engineering Structures*, **196**, 109278. <https://doi.org/10.1016/j.engstruct.2019.109278>
- ¹⁰ Rawat, A., Mittal, V., Chakraborty, T., & Matsagar, V. (2019). Earthquake induced sloshing and hydrodynamic pressures in rigid liquid storage tanks analyzed by coupled acoustic-structural and Euler-Lagrange methods, *Thin-Walled Structures*, **134**, 333–346. <https://doi.org/10.1016/j.tws.2018.10.016>
- ¹¹ Lyu, Y., Sun, J., Sun, Z., Cui, L., & Wang, Z. (2021). Seismic response calculation method and shaking table test of horizontal storage tanks under lateral excitation, *Earthquake Engineering & Structural Dynamics*, **50**(2), 619–634. <https://doi.org/10.1002/eqe.3349>
- ¹² Bakalis, K., & Karamanos, S. A. (2020). Uplift mechanics of unanchored liquid storage tanks subjected to lateral earthquake loading, *Thin-Walled Structures*, **158**, 107145. <https://doi.org/10.1016/j.tws.2020.107145>
- ¹³ Safari, S., & Tarinejad, R. (2016). Parametric study of stochastic seismic responses of base-isolated liquid storage tanks under near-fault and far-fault ground motions, *Journal of Vibration and Control*, **24**(24), 5747–5764. <https://doi.org/10.1177/1077546316647576>
- ¹⁴ Compagnoni, M. E., Curadelli, O., & Ambrosini, D. (2018). Experimental study on the seismic response of liquid storage tanks with Sliding Concave Bearings, *Journal of Loss Prevention in the Process Industries*, **55**, 1–9. <https://doi.org/10.1016/j.jlp.2018.05.009>
- ¹⁵ Cheng, X., Jing, W., Du, Y., Bao, C., & Wu, Z. (2018). Study on shock mitigation of concrete rectangular liquid storage structure with sliding shock insulator and limiting devices based on shaking table test, *China Civil Engineering Journal*, **51**(12), 120–132. <https://doi.org/10.15951/j.tmgcxb.2018.12.010>
- ¹⁶ Nikoomanesh, M. R., Moeini, M., & Goudarzi, M. A. (2019). An innovative isolation system for improving the seismic behaviour of liquid storage tanks, *International Journal of Pressure Vessels and Piping*, **173**, 1–10. <https://doi.org/10.1016/j.ijpvp.2019.04.012>
- ¹⁷ Kim, J. S., Jung, J. P., Moon, J. H., Lee, T. H., & Han, T. S. (2019). Seismic fragility analysis of base-isolated LNG storage tank for selecting optimum friction material of friction pendulum system, *Journal of Earthquake and Tsunami*, **13**(2), 1950010. <https://doi.org/10.1142/S1793431119500106>
- ¹⁸ Jiang, Y., Zhao, Z., R Zhang, Domenico, D. D., & Pan, C. (2020). Optimal design based on analytical solution for storage tank with inerter isolation system, *Soil Dynamics and Earthquake Engineering*, **129**, 105924. <https://doi.org/10.1016/j.soildyn.2019.105924>
- ¹⁹ Lv, Y., Sun, Z. G., Sun, J. G., Cui, L. F., & Wang, Z. (2020). Dynamic analysis of rolling isolation with variable curvature and application in spherical tanks, *Journal of Vibration Engineering*, **33**(1), 188–195. <https://doi.org/10.16385/j.cnki.issn.1004-4523.2020.01.021>
- ²⁰ Zhou, J. W., & Zhao, M. (2021). Shaking table test of liquid storage tank with finite element analysis considering uplift effect, *Structural Engineering and Mechanics*, **77**(3), 369–381. <https://doi.org/10.12989/sem.2021.77.3.369>
- ²¹ Krishnamoorthy, A. (2021). Finite element method of analysis for liquid storage tank isolated with friction pendulum system, *Journal of Earthquake Engineering*, **25**(1), 82–92. <https://doi.org/10.1080/13632469.2018.1498815>
- ²² Qi, Y. C., Qiu, H. X., & Ma, Y. Q. (2017). Experimental study and finite element analysis on the sloshing suppression in storage tank under seismic excitations, *Journal of Vibration and Shock*, **36**(2), 190–195. <https://doi.org/10.13465/j.cnki.jvs.2017.02.031>
- ²³ Cheng, X. S., Jing, W., & Gong, L. J. (2017). Simplified model and energy dissipation characteristics of a rectangular liquid storage structure controlled with sliding base isolation and displacement-limiting devices, *Journal of Performance of Constructed Facilities*, ASCE, **31**(5), 1–11. [https://doi.org/10.1061/\(ASCE\)CF.1943-5509.0001066](https://doi.org/10.1061/(ASCE)CF.1943-5509.0001066)
- ²⁴ Jing, W., Chen, P., & Song, Y. (2020). Shock absorption of concrete rectangular liquid storage tank with different kinds of isolation measures. *Earthquakes and Structures*, **18**(4), 467–480. <https://doi.org/10.12989/eas.2020.18.4.467>